

3D vessel extraction in the rat brain from Ultrasensitive Doppler images

E. Cohen, T. Deffieux, C. Demené, L. D. Cohen, and M. Tanter

Abstract Ultrasensitive Doppler is a recent medical imaging technique enabling high sensitive acquisition of blood flows which can detect small vascular features without contrast agents. Applied to cerebral tomographic imaging of rodents, this method produces very fine vascular 3D maps of the brain at high spatial resolution of 100 μm . These vascular networks contain characteristic tubular structures that could be used as landmarks to localize the position of the ultrasonic probe and take advantage of the easy-to-use property of ultrasound devices. In this study, we propose a computational method that performs 3D extraction of vascular paths and estimates effective diameters of vessels, from Ultrasensitive Doppler 3D reconstructed images of the rat brain. The method is based on the Fast Marching algorithm to extract curves minimizing length according to a relevant metric.

1 Introduction

1.1 Context

Medical ultrasound imaging has become a major clinical technique achieving an anatomical imaging of high quality, usually associated to a Doppler examination for blood flows observation and quantification. Ultrasound devices are also very convenient tools thanks to their portability, real time working and low-cost. Today, the

E. Cohen, T. Deffieux, C. Demené, and M. Tanter
Institut Langevin, ESPCI ParisTech, PSL Research University, CNRS, UMR 7587, INSERM U979, 75005 Paris, France
e-mail: {emmanuel.cohen, thomas.deffieux, charlie.demene, mickael.tanter}@espci.fr

E. Cohen, and L. D. Cohen
University Paris Dauphine, PSL Research University, CNRS, UMR 7534, CEREMADE, 75016 Paris, France
e-mail: emmanuel.cohen@dauphine.eu, cohen@ceremade.dauphine.fr

observation of very fast variations in the human body like mechanical waves propagation [8] or fast blood flows [2] is possible by ultrafast ultrasound imaging. Instead of using line-per-line focusing of ultrasonic beams like in standard ultrasound imaging, ultrafast imaging uses ultrasonic plane-wave transmissions associated to the power of graphical processing unit based platforms, in order to accelerate typical frame rates to more than 1000 frames per second [12]. Ultrasensitive Doppler is one of these new ultrasensitive techniques which allows high sensitive acquisition of small vascular features without contrast agent.

Ultrasensitive Doppler imaging produces very fine 3D vascular maps of the rodent brain with high spatial resolution. The acquisition is realized in vivo thanks to a simple mechanical system described in [6]. A mechanical scanning process acquires successive 2D sections along the rodent brain surface for several different orientations. Using a tomographic approach, a post-processing treatment of the data reconstructs a real 3D volume of the cerebral vascular network.

1.2 Motivations

The cerebral vascular network may serve as landmark in the brain for many purposes: real time neuronavigation, neurosurgery monitoring, brain tumor monitoring, etc. For instance, in Cohen et al. [3], we have proposed such a system to neuronavigate the rodent brain in real time. We successfully registered different ultrasensitive Doppler 3D scans using the cerebral vascular print as a matching feature. The algorithm used compares 2D brain sections by correlation, demonstrating the amount of positioning information contained by the ultrasensitive Doppler signal. Besides, this new real time neuronavigation system based on ultrasounds is of great interest given the easy-to-use properties of ultrasound devices: portability, real time, low cost, etc.

Consequently, we envisage to extract some geometric features characterizing the cerebral vascular network from ultrasensitive Doppler 3D images. Indeed, a finer description of the vascular print will lead to a better understanding and analysis

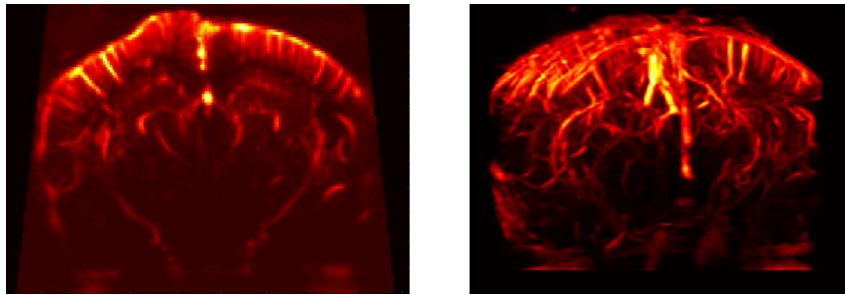


Fig. 1 Ultrasensitive Doppler imaging of the rat brain. Left: 2D ultrasensitive Doppler coronal plane. Right: 3D tomographic reconstruction [6].

of the vasculature; in addition, it will serve as a more accurate matching feature in all registration tasks aiming to find invariant cerebral vascular structures. In the present study, we propose a computational method that performs 3D extraction of vascular paths from tomography based 3D reconstruction of the rat brain by ultrafast ultrasound imaging [6]. In order to distinguish between small and large vessels, the method also enables the estimation of vessel diameters.

2 Material and methods

2.1 Material

In vivo experiments were performed on anesthetized rats using ultrasensitive Doppler. Ultrafast ultrasonic imaging enables fast acquisition of brain sections at $100\mu\text{m} \times 100\mu\text{m}$ resolution in the image plane. A 15MHz motorized probe acquires $400\mu\text{m}$ -thick brain sections with $200\mu\text{m}$ spacing. A typical 3D scan of the total width of the rat brain along one specific direction contains around 65 sections. A tomographic reconstruction can be achieved from several scan acquisitions along 18 different orientations, to obtain 3D high spatial resolution volume of around $200 \times 300 \times 300$ pixels of size $100\mu\text{m} \times 100\mu\text{m} \times 100\mu\text{m}$. A complete description of the experimental set up can be found in [6].

2.2 Minimal path extraction

The problem of extracting the minimal path between two points $\mathbf{x}_0, \mathbf{x}_1 \in \Omega \subset \mathbb{R}^d$ ($d = 2, 3$) in an image consists in finding the curve joining them and following the shortest possible path. The definition of a shortest path is generally associated to the Euclidean metric (or distance) $d_e(\mathbf{x}_0, \mathbf{x}_1) = \langle \mathbf{x}_1 - \mathbf{x}_0, \mathbf{x}_1 - \mathbf{x}_0 \rangle^{1/2}$ leading to the segment joining \mathbf{x}_0 and \mathbf{x}_1 for the minimal path. However, in an image, a segment

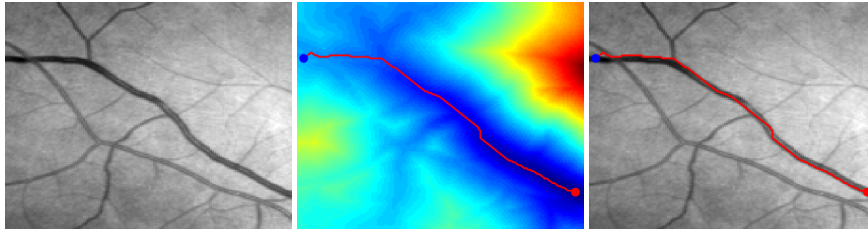


Fig. 2 Illustration of the minimal path extraction technique used on a 2D retina image. From left to right: the original image; the geodesic distance map corresponding to the red start point; the minimal path solution with the blue point as destination.

does not generally suite to represent the path between two points (see for instance the extraction of a retina vessel on figure 2).

Therefore, one can introduce a Riemannian metric that locally depends on the pixel intensity in order to make shortest paths depend on the most salient variations of the image, as it is well explained in [10]. Let $\gamma: [0, 1] \rightarrow \mathbb{R}^d$ be a smooth curve joining $\gamma(0) = \mathbf{x}_0$ to $\gamma(1) = \mathbf{x}_1$, a Riemannian metric or geodesic distance can be defined as

$$d(\mathbf{x}_0, \mathbf{x}_1) = \min_{\gamma} L(\gamma),$$

where $L(\gamma)$ is the Riemannian curve length of γ , and is given by

$$L(\gamma) = \int_0^1 \langle \gamma'(t), W(\gamma(t)) \gamma'(t) \rangle^{1/2} dt.$$

As expected, the metric is now a function of a saliency map $W: \mathbb{R}^d \rightarrow \mathbb{R}$ called potential, that should be chosen low in the image areas to be extracted. In general, W is a symmetric positive tensor field of $\mathbb{R}^{d \times d}$ but we restrain our study to the isotropic case. In fact, to extract vessels, we will build W from the intensity of the blood flow which is a scalar function of the 3D space.

From then on, the minimal path extraction problem is to solve the following minimization problem

$$\gamma^* = \arg \min_{\gamma} L(\gamma). \quad (1)$$

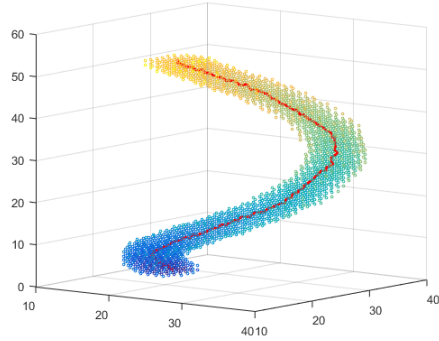
Given any set S of start points, one can define the geodesic distance map by

$$U_S(\mathbf{x}) = \min_{\mathbf{x}_0 \in S} d(\mathbf{x}_0, \mathbf{x}).$$

As described in [4, 10], if we manage to compute U_S , the solution of the problem (1) satisfies the following gradient descent

$$\frac{d\gamma^*(t)}{dt} = - \frac{\nabla U_S(\gamma^*(t))}{\|\nabla U_S(\gamma^*(t))\|}. \quad (2)$$

Fig. 3 Illustration of the minimal path extraction technique used on a 3D synthetic helical structure. The start and destination points are respectively chosen at the bottom and top of the helice. The color map follows the values of the geodesic distance map.



The computation of U_S is a more complicated. From results on the viscosity solution of the Hamilton-Jacobi equation [5, 10], it can be proved, under assumptions of compactness and continuity respectively for S and W , that U_S is the unique viscosity solution of the Eikonal equation

$$\begin{cases} \|\nabla U_S(\mathbf{x})\| = W(\mathbf{x}), \forall \mathbf{x} \in \Omega \\ U_S(\mathbf{x}) = 0, \forall \mathbf{x} \in S \end{cases} . \quad (3)$$

Some geometric interpretations can also be found in [4] and serve as elements of proof for better understanding.

To solve numerically the Eikonal equation, we use the Fast Marching Method (FMM) introduced by Sethian [11] and we follow the numerical scheme presented in [7] for 3D images ($d = 3$). The FMM is a front propagation approach computing iteratively the values of U_S in increasing order. Then, we extract γ^* by using a simple discrete gradient descent to solve (2) avoiding angular error accumulation [4]: from the destination point \mathbf{x}_1 , the back propagation follows the direction of the lowest U_S value of a regular neighbor grid around the current iteration point, until the first start point \mathbf{x}_0 is reached i.e. as soon as $U_S(\mathbf{x}) = 0$.

Illustrations of the method just described in 2D and 3D are shown on figures 2 and 3.

2.3 Iterative keypoint detection

In the case of vessel extraction and particularly when a large amount of vessels constitutes a complex vascular network, it is convenient to extract the desired vessels from a unique start point. Indeed, because of bifurcations of vessels, it would require many different unknown pairs of start and destination points of the minimal path extraction method described just before.

Therefore, we use the Minimal Path method With Keypoint Detection (MPWKD) introduced by [1]. From a single start point \mathbf{x}_0 and given a parameter λ , intermediate points, called keypoints, are successively detected along the curve of interest with a spacing between them almost constant to λ . Another advantage of this method is the influence of λ on the path when the potential is too noisy or not enough contrasted; in this case, small values of λ can prevent minimal path solution from wrong shortcuts to the start point [1].

Like FMM, the MPWKD algorithm is based on minimal path extraction technique described in 2.2. The geodesic distance map $U_{\mathbf{x}_0}$ is first computed until the front reaches a keypoint \mathbf{p}_0 with an Euclidean distance higher than λ . Then, the front continues to propagate considering \mathbf{p}_0 as a new start point, i.e. $S = \{\mathbf{x}_0, \mathbf{p}_0\}$ and $U_S(\mathbf{p}_0) = 0$, until a new keypoint \mathbf{p}_1 again with an Euclidean distance higher than λ . The algorithm iterates this procedure until the approximated total Euclidean length of the path is higher than a second parameter L to obtain a quasi equidistant set of keypoints \mathbf{p}_i . The Euclidean distance map is computed just as the geodesic by

solving (3) with $W(\mathbf{x}) = 1$ for all $\mathbf{x} \in \Omega$. The extraction of the total minimal path is performed at each iteration after which a new keypoint is detected by the same simple gradient descent on U_S as in 2.2. The MPWKD is also taking into account the number of adjacent Voronoi regions in order to extract the correct path.

2.4 Vessel effective diameter estimation

From the previous analysis, the obtained minimal path extraction can be viewed as a graph representation of the vascular network. The keypoints would be the nodes of the graph and an edge would be defined by the path connecting two successive keypoints. This graph description may be particularly useful to compare different cerebral vascular networks.

As a first step leading to a suitable graph representation of the cerebral vascular network, we propose to distinguish vessels according to their effective diameters. Indeed, the size of the vessels is a crucial feature useful to characterize different kind of vascular structures in relation with some physiological parameters such as blood flow velocity, pressure, etc. In the context of ultrafast Doppler imaging, due to the physics of ultrasound devices, the observed size of vessels is not rigorously their real size. That is why we will deal here with effective diameters of vessels.

The previous extracted minimal paths are supposed to be localized inside the vessels, even if they are not a priori centered on their centerlines [10]. Thus, at each point of the extracted minimal paths, one can consider the orthogonal plane to the vessel and passing through this point. In this plane, if we model a vessel by a curvilinear and tubular structure, the point of interest should be located inside a group of pixels fitting an ellipse. The vessel diameter is then estimated by the characteristic size of the latter ellipse.

Computing the orthogonal plane requires to know precisely the local orientation of the vessel. A simple faster method consists in considering the best approximation of the orthogonal plane among the local coronal, sagittal and horizontal sections. This is done by fitting an ellipse or basically a circle in each of those three planes and selecting the smallest one as the correct circle estimate (see figure 4); in fact,

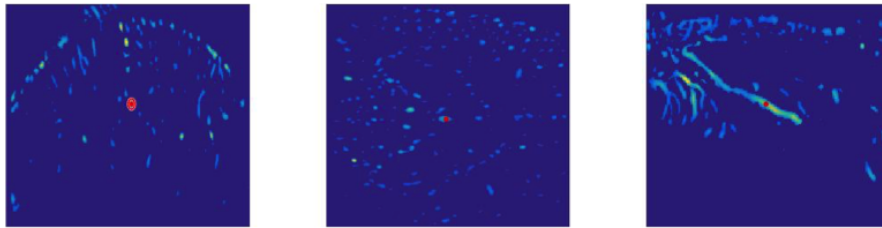


Fig. 4 Vessel effective diameter estimation method. From left to right: coronal, horizontal and sagittal planes that locally intersect the minimal path at the red point. In this example, the smallest fitted circle is on the coronal plane.

the two other bigger estimates fit actually non-circular structures revealing the non-orthogonality to the vessel. Finally, the center of the fitted circle allows to recenter the point of interest and thus the minimal path at the center of the vessel.

3 Results and discussion

In order to show the efficacy of the proposed method, we first apply it on a 2D coronal plane of the rat brain (fig. 6), obtained by averaging 30 successive coronal sections of the 3D ultrafast Doppler tomographic reconstruction presented in 2.1. A Doppler image shows the intensity of the blood flow which is maximal at the center of the vessels. Therefore, the metric should be simply chosen as an inversely proportional function to the image. A first simple and successful model corresponds to $W = 1/I$ where I is the 2D or 3D ultrafast Doppler image. Before launching the keypoints detection algorithm (see 2.3), one must take into account the image background the presence with many pixels of very low intensity that do not correspond to vessels. Otherwise, the MPWKD finds many outlier keypoints. The left image of figure 5 illustrates this over-detection result. Then, the middle image shows the MPWKD performance after a thresholding of the data: a large part of the vascular network is well extracted revealing the importance of the pre-processing segmentation step of the image. The right image shows how to get better performance by performing before the thresholding step a histogram equalization based on [13] in order to increase the contrast and then enhance vascular structures. This time, almost all the 2D vascular tree is extracted even the deepest vessels of the brain. In all these simulations, the start point from which the MPWKD starts the keypoint detection is red colored and chosen in an image area of highest intensity like the vertical central vessel located on the symmetry axis of the brain. One can appreciate the enhancement of the vascular structures of the image on figure 6. The two last images of figure 6 show the Euclidean distance map updated at each keypoint detection and the approximated total Euclidean length.

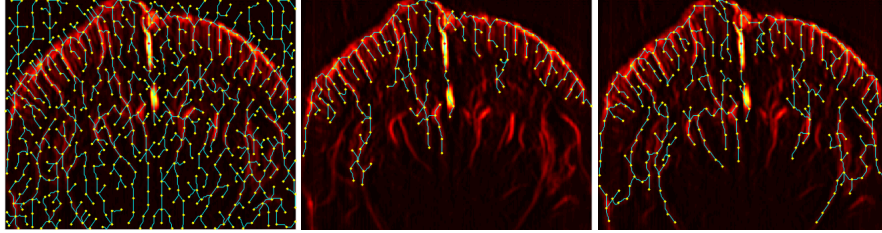


Fig. 5 Minimal path extraction with keypoint detection in 2D. From left to right, the method is applied to: original image; image after thresholding; image after thresholding and histogram equalization. Start points, keypoints, and minimal paths are respectively marked in red, yellow, and cyan.

The proposed method was then tested in 3D on a tomographic reconstruction of the rat brain (see 2.1). In real 3D data, the observed vascular structures are much more consistent with the real vasculature, which was not the case in 2D average of several successive planes where wrong superimposition and then bifurcations of vessels could appear. That is why the MPWKD produces a very nice 3D vascular network extraction even without thresholding of the data (fig. 7). One can observe the profusion of extracted vessels in particular the high number of short vessels that makes difficult the physical interpretation and validation of the result. In order to refine the extraction, a pre-processing step to segment the more significant vascular structures can be applied. For instance, we used the Optimally Oriented Flux (OOF) filter proposed by [9] for curvilinear structure detection. Figure 8 illustrates the 3D segmentation of the data by OOF. Many noisy pixels are changed to zero and the surface of vessels is more accurately delimited. However, when the MPWKD is directly applied on the segmented volume, fewer keypoints are detected and one may repeat the keypoint detection algorithm from different start points to get the whole vascular tree.

The OOF filter is particularly useful for the vessel effective diameter estimation (see 2.4). Indeed, in order to get consistent circle fitting like on figure 4, the vessel section containing the red point should be composed of almost exclusively pixels of interest, since the algorithm estimating the diameter only counts those pixels to define the area of the vessel section. If this area is not well delimited, then many outlier pixels will lead to a wrong estimated area. Thus, after delimiting vessels by

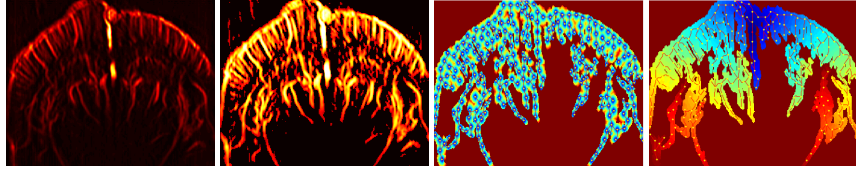


Fig. 6 From left to right: 2D ultrasensitive Doppler; thresholding and histogram equalization of the previous image; updated Euclidean distance map; approximated total Euclidean length map.

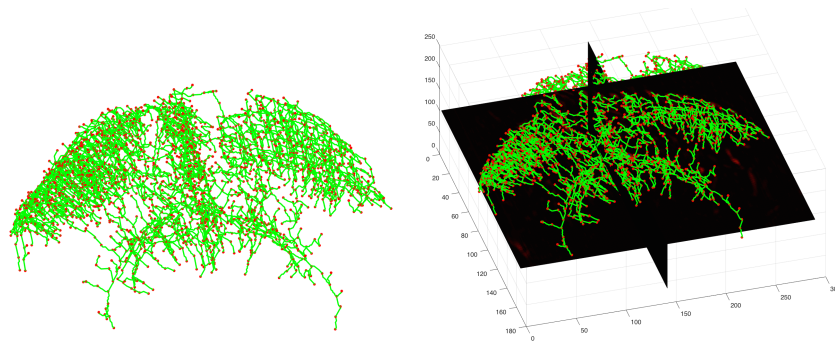


Fig. 7 Minimal path extraction with keypoint detection in 3D. Start points, keypoints, and minimal paths are respectively marked in blue, red, and green.

OOF and using the vascular tree obtained by MPWKD on original data, we obtain a color map of the estimated vessel diameters as shown on figure 9. One can observe the profusion of small vessels that ultrafast ultrasound imaging enables to detect.

4 Conclusion

In this study, we have presented a first computational method capable of analyzing the vasculature of the rat brain from 3D ultrasensitive Doppler. The proposed method has the advantage to be really fast (tens of seconds), implementing the solution with C++. Future work should improve several issues: the accuracy of the minimal path extraction by considering anisotropic metrics and studying the influence of the distance parameter between the keypoints; the enhancement of vascular

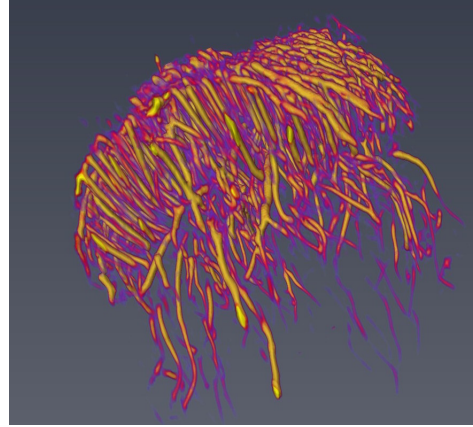


Fig. 8 Vascular segmentation in 3D by the Optimally Oriented Flux filter.

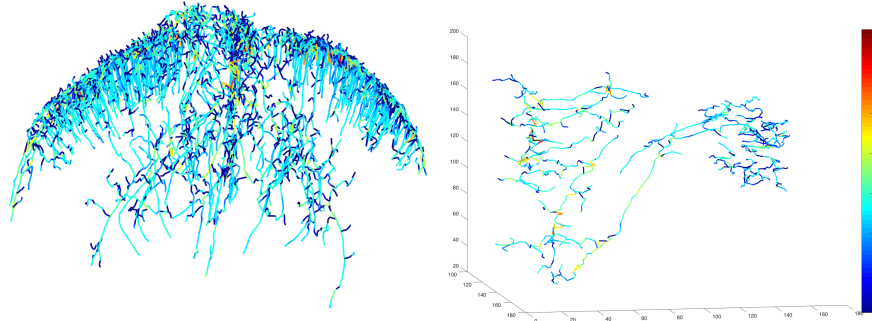


Fig. 9 Vessel effective diameter estimation. Left: vessel diameters of the whole extracted vascular network. Right: vessel diameters of a partial vascular network computed by MPWKD after OOF filtering (the forebrain is on the left of the graph). The range of the color map values is from 0 (blue) to 7 (red) pixels.

structures to improve the quality of the extracted vascular tree; and finally, the accuracy of the proposed vessel diameter estimation by considering local orthogonal planes to vessels.

References

1. Benmansour, F., Cohen, L.D.: Fast object segmentation by growing minimal paths from a single point on 2d or 3d images. *Journal of Mathematical Imaging and Vision* **33**(2), 209–221 (2009)
2. Bercoff, J., Montaldo, G., Loupas, T., Savery, D., Meziere, F., Fink, M., Tanter, M.: Ultrafast compound doppler imaging: providing full blood flow characterization. *IEEE transactions on ultrasonics, ferroelectrics, and frequency control* **58**(1), 134–147 (2011)
3. Cohen, E., Deffieux, T., Tiran, E., Demene, C., Cohen, L., Tanter, M.: Ultrasensitive doppler based neuronavigation system for preclinical brain imaging applications. In: *Ultrasonics Symposium (IUS), 2016 IEEE International*, pp. 1–4. IEEE (2016)
4. Cohen, L.D., Kimmel, R.: Global minimum for active contour models: A minimal path approach. *International journal of computer vision* **24**(1), 57–78 (1997)
5. Crandall, M.G., Lions, P.L.: Viscosity solutions of hamilton-jacobi equations. *Transactions of the American Mathematical Society* **277**(1), 1–42 (1983)
6. Demené, C., Tiran, E., Sieu, L.A., Bergel, A., Gennisson, J.L., Pernot, M., Deffieux, T., Cohen, L., Tanter, M.: 4d microvascular imaging based on ultrafast doppler tomography. *NeuroImage* **127**, 472–483 (2016)
7. Deschamps, T., Cohen, L.D.: Fast extraction of minimal paths in 3d images and applications to virtual endoscopy. *Medical image analysis* **5**(4), 281–299 (2001)
8. Gennisson, J.L., Deffieux, T., Fink, M., Tanter, M.: Ultrasound elastography: principles and techniques. *Diagnostic and interventional imaging* **94**(5), 487–495 (2013)
9. Law, M.W., Chung, A.C.: Three dimensional curvilinear structure detection using optimally oriented flux. In: *European conference on computer vision*, pp. 368–382. Springer (2008)
10. Peyré, G., Péchaud, M., Keriven, R., Cohen, L.D.: Geodesic methods in computer vision and graphics. *Foundations and Trends® in Computer Graphics and Vision* **5**(3–4), 197–397 (2010)
11. Sethian, J.A.: *Level set methods and fast marching methods: evolving interfaces in computational geometry, fluid mechanics, computer vision, and materials science*, vol. 3. Cambridge university press (1999)
12. Tanter, M., Fink, M.: Ultrafast imaging in biomedical ultrasound. *IEEE transactions on ultrasonics, ferroelectrics, and frequency control* **61**(1), 102–119 (2014)
13. Zuiderveld, K.: Graphics gems iv. chap. Contrast Limited Adaptive Histogram Equalization, pp. 474–485. Academic Press Professional, Inc., San Diego, CA, USA (1994). URL <http://dl.acm.org/citation.cfm?id=180895.180940>